A Study on the Aerodynamic Properties of a Canard-Configuration WISES

by Yuma Ito* and Hidetsugu Iwashita
Graduate School of Engineering, Hiroshima University, Hiroshima, Japan
E-mail: m124699@hiroshima-u.ac.jp

Highlights:

- Boundary Element Method (BEM) is applied to the lifting body problem, and nonlinear phenomena with free-surface interaction effect and wake influence are made clear by numerical calculations.
- Aerodynamics of wings with and without end-plates and the aerodynamic interaction effect between propulsor and whole airframe are investigated by the wind tunnel experiment. Results are compared with computational results for the validation.

1 Introduction

When wings fly in the vicinity of the ground or the sea surface, their aerodynamic performance improves remarkably. This phenomenon is called " Ground Effect ". WISES (Wing-In-Surface-Effect Ship) and/or WIG (Wing-In-Ground effect) is an unconventional ship or aircraft expected to be a high-speed transportation system utilizing the ground effect.

So far, many researches on WIG have been carried out. Most of them focus on the steady problem of WIG flying over a flat ground [1] and simple rectangular wings are used in the studies. More practical studies can be seen in Iwashita et al. [2][3]. They studied both the steady and unsteady problems of a canard-configuration WIG [4] flying over the calm water and progressive waves, and made clear the aerodynamic interaction effect between the front wing and the main wing with end-plates. However, the water surface is treated as a rigid surface and the nonlinear effect of the roll-up of the wake sheet behind the wing is omitted in their theoretical calculations.

In the present study, the free surface effect generated by WIG in the aerodynamics and the wake roll-up in the ground effect are investigated. Numerical and experimental studies are performed not only for the main wing with complicated profile but also for the whole airframe. The aerodynamic interaction effect between the propulsor and the airframe is also discussed.

2 Formulation

We consider a wing flying at constant forward speed U in an incompressible, inviscid and irrotational air domain, and take a body-fixed coordinate system as illustrated in figure 1. S_H, S_F and S_W represent the wing surface, the free surface and the wake surface respectively. The normal vector $\boldsymbol{n}$ is taken to point inward the air domain. Free surface is treated as a rigid surface and wake sheet flows out along the uniform flow. Then the velocity potential Φ of the air governed by the Laplace equation is expressed in the form,

$$\Phi(x,y,z) = U[-x + \phi(x,y,z)] \qquad (1)$$

In the first step of the following iteration process, the perturbation velocity potential $\phi(x,y,z)$ must satisfy the following boundary conditions:

$$[H] \quad \frac{\partial \phi(x,y,z)}{\partial n} = n_x \qquad \text{on } S_H \qquad (2)$$

$$[F] \quad \frac{\partial \phi(x,y,z)}{\partial n} = 0 \qquad \text{on } S_F(z=0) \qquad (3)$$

$$[K] \quad p^+ - p^- = 0 \qquad \text{on } S_W \qquad (4)$$

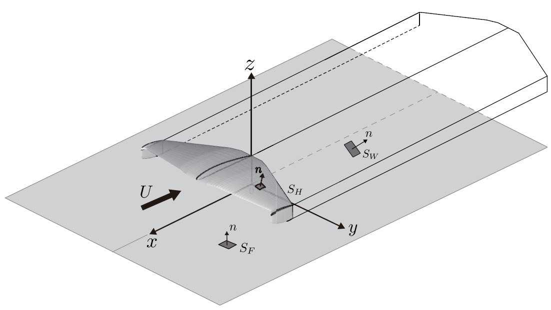

Fig. 1: Coordinate system.

Equation (4) represents the Kutta condition where p^+ and p^- indicate the pressures on upper and lower surface of the wake sheet. By applying Green's second identity, we obtain the following integral equation with respect to ϕ:

$$\frac{\phi(P)}{2} - \iint_{S_H+S_F} \frac{\partial G_0(P,Q)}{\partial n_Q}\phi(Q)\, dS - \iint_{S_W} \left[\phi(Q_T^+) - \phi(Q_T^-)\right] \frac{\partial G_0(P,Q)}{\partial n_Q}\, dS$$
$$= -\iint_{S_H+S_F} \frac{\partial \phi(Q)}{\partial n_Q} G_0(P,Q)\, dS\,, \quad P \in S_H + S_F(z=0) \qquad (5)$$

where $G_0(P,Q) = 1/4\pi|PQ|$, $P = (x, y, z)$ and $Q = (x', y', z')$. $\phi(Q_T^+)$ and $\phi(Q_T^-)$ show the velocity potentials of upper and lower point at the trailing edge, Q_T^+ and Q_T^-. Kutta condition including the nonlinear term,

$$\frac{p - p_0}{\rho_a U^2/2} = 2\frac{\partial \phi}{\partial x} - \nabla\phi \cdot \nabla\phi \tag{6}$$

is numerically satisfied by applying the Newton-Raphson method. p_0 is an atmospheric pressure and ρ_a is a density of the air. The integral equation (5) is discretized into a finite number of elements and numerically solved based on the constant panel method. The velocity field $\nabla\phi$ on the wing surface and the free surface $(z = 0)$ is calculated by the numerical derivative method (2D Spline interpolation).

Once we obtain ϕ on S_H and S_F, we can evaluate the pressure distribution on $S_F(z = 0)$ by equation (6). Assuming an incompressible, inviscid and irrotational fluid, we can introduce the velocity potential for the fluid defined as $\Phi_w = U[-x + \phi_w]$. Linearization of the free surface boundary condition leads to the following condition and the wave elevation on $z = 0$:

$$\frac{\partial^2 \phi_w}{\partial x^2} + K_0 \frac{\partial \phi_w}{\partial z} = \frac{1}{2}\Big(\frac{\rho_a}{\rho_w}\Big)\frac{\partial}{\partial x}\Big(\frac{p - p_0}{\rho_a U^2/2}\Big), \quad \zeta = \frac{1}{K_0}\Big\{\frac{\partial \phi_w}{\partial x} - \frac{1}{2}\Big(\frac{\rho_a}{\rho_w}\Big)\Big(\frac{p - p_0}{\rho_a U^2/2}\Big)\Big\} \quad \text{on } z = 0 \tag{7}$$

where $K_0 = g/U^2$ and ρ_w is a density of the fluid. By solving the boundary value problem on ϕ_w by means of the Rankine panel method, the wave elevation ζ is obtained. In the second step, the air domain is solved again after replacing equation (3) with a new condition $\partial\phi/\partial n = n_x$ on $S_F(z = \zeta)$. Aerodynamics acting on the wing in the second step is compared with that obtained in the first step. Thus we can confirm the effect of the free surface generated by the wing in aerodynamics of the wing.

In this study, we also carry out the time domain calculation in order to investigate the effect of the wake roll-up in the aerodynamics. A space-fixed coordinate system is taken as illustrated in figure 2. The free surface is assumed to be rigid and flat. We solve the boundary value problem expressed in equations (1) $\sim$ (4) in advance, and obtained solution is set to a solution of $t = 0$. When we solve this problem, G_0 in equation (5) is replaced by $G(P, Q)$ taking the mirror image into account, which is defined in equation (12), and the wake sheet is assumed to flow out along the uniform flow.

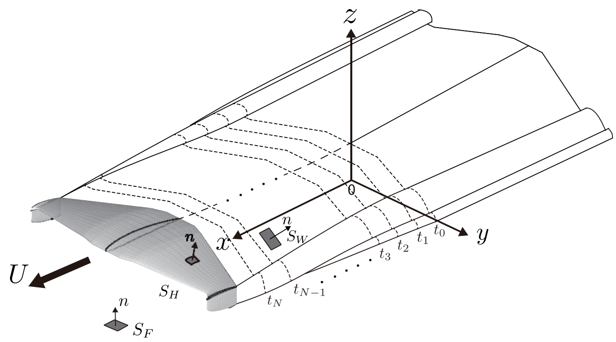

Fig. 2: Coordinate system for time domain BEM.

After $t = 0$, the wing advances at constant forward speed U with adding wake-sheet element of length $U\Delta t$. The velocity potential $\Phi(x, y, z; t)$ is solved so that the following conditions are satisfied at each time step:

$$[H] \qquad \frac{\partial \Phi(x, y, z; t)}{\partial n} = U n_x \qquad \text{on } S_H \tag{8}$$

$$[F] \qquad \frac{\partial \Phi(x, y, z; t)}{\partial n} = 0 \qquad \text{on } S_F(z = 0) \tag{9}$$

$$[K] \qquad p^+(x, y, z; t) - p^-(x, y, z; t) = 0 \qquad \text{on } S_W \tag{10}$$

The integral eqation with respect to Φ is expressed in the form,

$$\frac{\Phi(P;t)}{2} - \iint_{S_H(t)} \frac{\partial G(P,Q)}{\partial n_Q}\Phi(Q;t)\,dS = -\iint_{S_H(t)} \frac{\partial \Phi(Q;t)}{\partial n_Q} G(P,Q)\,dS$$
$$+ \int_0^t \Big\{\iint_{S_W(t)} \big[\Phi(Q_T^+;\tau) - \Phi(Q_T^-;\tau)\big]\frac{\partial G(P,Q)}{\partial n_Q}\,dS\Big\}\,d\tau\,, \quad P \in S_H \tag{11}$$

where
$$G(P,Q) = \frac{1}{4\pi}\left(\frac{1}{r} + \frac{1}{r'}\right), \quad \left.\begin{matrix} r \\ r' \end{matrix}\right\} = \sqrt{(x - x')^2 + (y - y')^2 + (z \mp z')^2} \tag{12}$$

Once we obtain Φ on S_H at each time step, we can evaluate the velocity field over the wake sheet by

$$\nabla\Phi(P) = -\iint_{S_H(t)} \Big\{\frac{\partial \Phi(Q;t)}{\partial n_Q}\nabla G(P,Q) - \nabla\frac{\partial G(P,Q)}{\partial n_Q}\Phi(Q;t)\Big\}$$
$$+ \int_0^t \Big\{\iint_{S_H(t)} \big[\Phi(Q_T^+;\tau) - \Phi(Q_T^-;\tau)\big]\nabla\frac{\partial G(P,Q)}{\partial n_Q}\Big\}\,d\tau\,, \quad P \in S_W \tag{13}$$

All the node points on the wake sheet are moved by using these velocities at each time step. Thus the deformation of the wake sheet and its effect in aerodynamics can be analyzed by the time marching calculation.

3 Numerical and Experimental Results

3.1 Free-surface interaction effect

We carried out the calculation following the formulation explained in the former part of the previous section in order to investigate the free-surface interaction effect in aerodynamics of WIG. The wing is a main wing of the canard-configuration WIG shown in Fig. 6. The wing section is NACA3409, chord length c is 0.7 m, span is 1.4 m and cathedral angle is 8 degrees. The end-plates are attached at both wing tips to improve the ground effect. Calculation conditions are $F_n = 7.6$, angle of attack $\alpha = 3$ degrees. and flight altitude h measured at the trailing edge is $h/c = 0.35$. Figure 3 shows the perspective view of the steady wave generated by the wing. Steep waves induced by the negative pressure due to the wing can be observed behind wing tips. However, the wave amplitude is smaller than 2 mm and not remarkable. As a result, the steady wave does not affect the aerodynamics of the wing as shown in the right figure. The frictional drag contained in C_D is computed by a commercial CFD software, ANSYS Fluent.

3.2 Wake roll-up effect

The time-domain calculation explained in a latter half of the previous section is performed in order to investigate the wake roll-up effect in aerodynamics. The left figure in 4 shows the deformation of the wake sheet behind the wing. Two roll-ups of the wake sheet can be confirmed at wing tip and end-plate tip, and the former is dominant. The wake sheet spreads to the span direction due to the presence of the ground. The pressure distributions on the wing sections are illustrated in the right figure comparing two calculations, namely, the calculation with free wake sheet and the calculation with the fixed wake sheet which flows out along the uniform flow. The deference is quite small and it can be concluded that wake roll-up effect in aerodynamics is negligible.

3.3 Aerodynamic properties of the main wing

A typical aerodynamic property of the main wing is shown in figure 5. Experiments were carried out using the wind tunnel in RIAM, Kyushu University. The lift-to-drag ratio increases as the altitude h/c becomes smaller. End-plates improve the ratio about 10 % at $h/c = 0.35$.

3.4 Aerodynamics of the canard-configuration WIG

We have also carried out the numerical and experimental study for the whole airframe model shown in figure 6. The interaction effect of the propulsor and the airframe is discussed mainly. These are presented in the workshop together with the details omitted in this abstract for lack of space.

REFERENCE

1) Rozhdestvensky, K.：Aerodynamics of a Lifting System in Extreme Ground Effect, 1st edition, Spring-Varlag.

2) Iwashita, H., Tanaka, S., et al. 2004, A Study on the Aerodynamic Interaction of Wings and the Aerodynamic Properties of a Canard-Configuration WISES Flying over Still Water and Waves (Part1), Journal of the Society of Naval Architects of Japan, Vol.194, pp.31-46

3) Iwashita, H. 2004, A Study on the Aerodynamic Interaction of Wings and the Aerodynamic Properties of a Canard-Configuration WISES Flying over Still Water and Waves (Part2), Journal of the Society of Naval Architects of Japan, Vol.194, pp.47-57

4) Akimoto, M., Kubo, S. et al. 2006, Flight Test of the Canard Type WISES by a Self Propulsion Model of 3.6m length, Journal of the Japan Society of Narval Architects and Ocean Engineers, Vol.3, pp.97-102

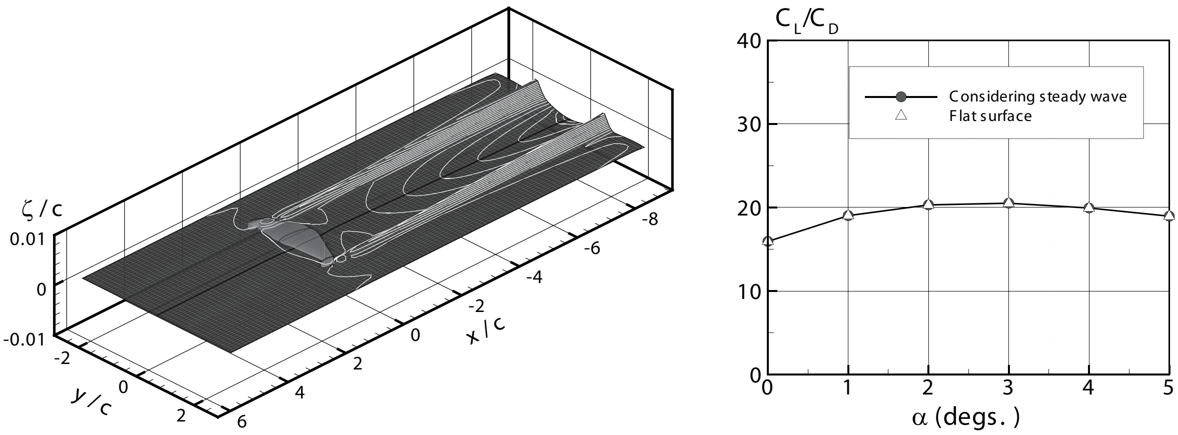

Fig. 3: Perspective view of the steady wave and aerodynamics of main wing with end-plates ($F_n = 7.6$, $\alpha = 3°$, h/c =0.35).

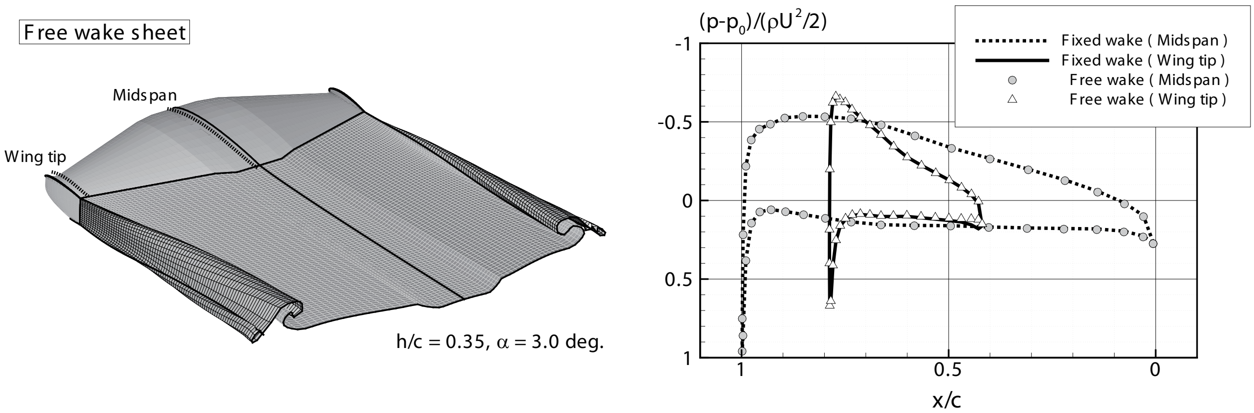

Fig. 4: Perspective view of wake deformation and 2-D pressure distributions ($\alpha = 3°$, h/c =0.35, $U = 20$ m/s, $\Delta t = 0.001$, time step = 85).

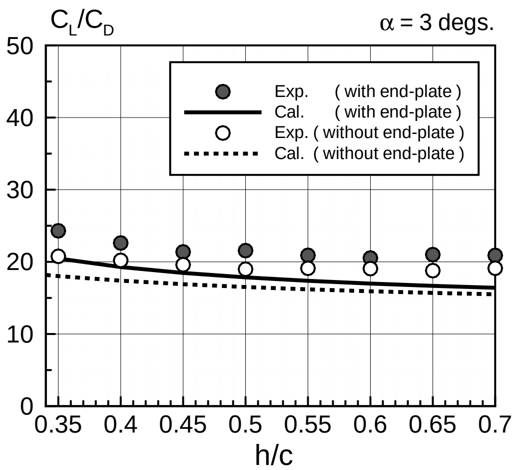

Fig. 5: Aerodynamic properties of the main wing with and without end-plates ($Re = 7.5 \times 10^5$).

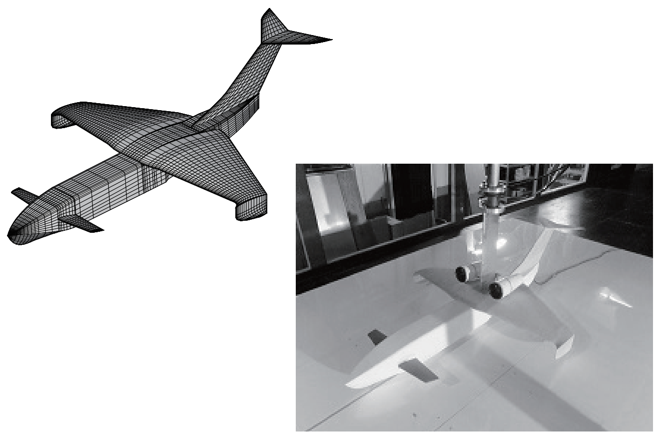

Fig. 6: Computational grid of whole airframe and experimental setup of a scale model.